Multifragment events in the $^{238}U+^{197}Au$ reaction at 15 MeV/nucleon

D. G. d'Enterria,[1] F. Fernández,[1] E. Luguera,[1] M. Debeauvais,[2] J. Ralarosy,[2] S. Jokic,[3] M. Zamani,[4] and J. Adloff[2]
[1]*Grup de Física de les Radiacions, Universitat Autònoma de Barcelona, 08193 Cerdanyola, Catalonia, Spain*
[2]*Centre de Recherches Nucléaires, 67037 Strasbourg, France*
[3]*University "Svetozar Markovic," 34000 Kragujevac, Yugoslavia*
[4]*University of Thessaloniki, 54006 Thessaloniki, Greece*
(Received 30 May 1995)

The $^{238}U+^{197}Au$ reaction has been studied at 15 MeV/nucleon bombarding energy. Correlations between two to seven final fragments with $Z \geq 8$ have been measured using CR-39 nuclear track detectors. An event-by-event kinematic analysis was carried out for three-body exit channel reactions which exhaust about half of the final fragment production cross section. Most of these ternary processes can be associated with intermediate and peripheral impact parameters. The dominant reaction mechanism is shown to be that of a first binary quasielastic or dissipative collision followed by the sequential binary fission of the excited quasi-U (or to a lesser extent of the excited target remnant). We observe also a net drift of nucleons from the target to the projectile prior to its decay.

PACS number(s): 25.70.−z, 25.70.Pq

I. INTRODUCTION

Nuclear reactions in heavy-ion collisions at intermediate energies (10–100 MeV/nucleon) have been widely studied both experimentally and theoretically over the last decade using varied projectiles and targets. Lately, the possibility of accelerating heavier projectiles to higher energies has allowed the study of highly excited nuclei with mass numbers $A > 200$. This fact, together with the development of almost 4π detectors capable of measuring exit channels of increasing multiplicity, has attracted interest in the evolution of the different reaction mechanisms and decay modes as a function of the excitation in these heavy systems. The purpose of our experiment was to investigate the characteristics of final fragment correlations in an intermediate-energy reaction with a very heavy ($A_p + A_t > 400$ u) projectile-target configuration at moderate excitation energies ($E^*_{\max} \approx 2.2$ MeV/nucleon), where the deexcitation process is expected to be dominated by sequential binary fission and/or light-particle evaporation [1]. More precisely, the present paper concentrates on the study of the mechanism of three-final-fragment production in the $^{238}U+^{197}Au$ reaction at 15 MeV/nucleon.

Several experiments [2–12] studying ternary and quaternary processes in very heavy nuclear reactions with uranium projectiles have been performed at bombarding energies below 10 MeV/nucleon. They show that in this low-energy regime the most probable reaction channels are one-neutron quasielastic transfer and sequential fission following a dissipative reaction with multinucleon transfer. In all these experiments the sequential fission of the ^{238}U projectile was observed with higher probability as the bombarding energy increased.

Heavy-ion collisions at 10–30 MeV/nucleon bombarding energy leading to three-body events have been usually interpreted in terms of an incomplete fusion process where only part of the projectile and target fuses to produce a transient dinuclear system. The subsequent evolution of the reaction, the reseparation and deexcitation of the system, has been described either from a high-energy point of view (participant-spectator picture) or from a low-energy one (deep inelastic dynamics plus fission). The former approach leads to the dynamic formation of a three-body final state (see, for example, [13]). In the latter scenario, either the slow or prompt sequential fissionlike decay of an excited projectilelike fragment issuing from a deep inelastic phase can also produce ternary events [14–18]. Other reactions do not have such a clear-cut production mechanism (see, for example, [19]).

Both the absence of similar studies in the intermediate-energy region with very heavy colliding nuclei like ^{238}U and ^{197}Au and the diversity of conclusions concerning the nature of the three-body events, where the question of the relative role of the instantaneous and sequential mechanisms is of major interest, have motivated our experiment. A heavy and quasisymmetric system such as $^{238}U+^{197}Au$ at moderate incident velocities ($\beta_{\text{proj}} \approx 0.177$) has two major advantages: it minimizes the preequilibrium emission of light charged particles and neutrons and favors the thermalization of the excitation energy produced in the collision. Moreover, since the reaction partners have nearly the same mass, on the average theoretically both should be equally excited.

In our experiment we used CR-39 solid state nuclear track detectors, which have been employed for the study of heavy fragments produced in low-, intermediate-, and high-energy nucleus-nucleus collisions [20–27]. All these different experiments have shown that CR-39 permits a good energy loss determination and an excellent spatial resolution of measured trajectories which makes it a fine tool for the study of heavy-multifragment emission phenomena. Its most important drawback, however, is that it requires individual track counting and thus the acquisition of statistically significant results is very time consuming.

The paper is organized as follows. In Sec. II the experimental techniques (including the setup and the kinematical reconstruction method for each ternary event) are described. Section III is devoted to the presentation and interpretation of the experimental results: first, global observables such as the reaction multiplicity and cross sections and secondly

other significant variables concerning three-body processes. The possible reaction mechanism and decay modes are discussed, the two-step nature of the ternary processes is established, and the fission properties of the system are treated. The summary of the experimental results is presented in Sec. IV.

II. EXPERIMENT

A. Setup

The experiment was performed using the incident ^{238}U beams delivered by the UNILAC accelerator at GSI in Darmstadt (Germany). The bombarding energy was 15 MeV/nucleon with fluences of 0.86×10^6 ions/cm^2. The targets consisted of layers of 1000 μg/cm^2 of ^{197}Au evaporated on one surface of the CR-39 track detector. The target thickness was determined with an accuracy of about 5%. The gold targets were bombarded perpendicular to their surfaces. This arrangement produced a 2π detection geometry in the laboratory system and an $\approx$100% efficiency in the case of our reaction. Eight different detector plates, each one with an area of 4×4 cm^2, were irradiated. A chemical development of the detectors was carried out in $5N$ NaOH at 60 °C for 120 min. These etching conditions produced well-developed tracks in the detector for each charged fragment ($Z\geq8$) in the angular range $\theta_{\rm lab}=3°-180°$, the threshold of detection being about 8 MeV cm^2/mg. Tracks shorter than 3 μm long were not detected. These limits prevented characterizing fragments with charges $Z<8$ [25]. More than 6×10^3 particle trajectories, produced in 2×10^3 interaction vertices with different fragment multiplicities, were scanned optically and measured. Determination of the ranges of the correlated particles, angles α_{ij} between them, and angles θ_i with respect to the incident beam direction were performed with an accuracy of ±1.5 μm and $\pm1.5°$, respectively.

To calculate the partial cross sections of our reaction, we have classified as three-body events all reactions having three detected fragments as well as those having two fragments with relative projected angle on the detection plane less than 180° (indirect or incompletely measured events). Due to momentum conservation and taking into account the angular error, these latter events were associated with a third fragment which escaped detection. Moreover, some four- and five-body events were found to be, respectively, five- and six-body events by the same analysis. The large solid angle coverage of our experimental arrangement strongly reduced the number of such incompletely measured events except in the case where the undetected charge was $Z<8$, and therefore yielded more reliable results than other less exclusive (though eventually more precise) experiments. In the ternary processes analysis, however, the background of incompletely measured events is understood to be subtracted and we have only considered those events with three heavy fragments detected (heavy fragments defined as nuclei with atomic number $Z\geq8$).

B. Kinematic reconstruction

A detailed kinematical analysis was made event by event for the three-body exit channel processes with the help of a FORTRAN code. In principle, ternary reactions are uniquely characterized by measuring the range of each final fragment, their emission angles, and the angles between them. Indeed, for each individual interaction the momentum p_i of each primary (i.e., before any eventual light-particle evaporation) fragment could be determined by solving momentum conservation equations in the lab frame, knowing the emission angles θ_i ($i=1,2,3$) with respect to the beam axis and the angles α_{ij} between tracks. The mean error of each momentum p_i was $\pm0.05p_i$ (MeV/c). The charge Z_i of each detected heavy product was then determined from the value of its momentum p_i and its experimentally measured range R_i in the detector. For each fragment a comparison was made between these two parameters and those derived from the range-energy curves in CR-39 calculated by the code TRIM-90 [28]. To compute the ion's incident energy E_i we assumed the mass number A_i of each produced fragment to be in the valley of stability (which is a reasonable supposition within our experimental precision). With TRIM-90 we constructed six-degree polynomial parametrizations of the path length R_i of all charges Z_i ($Z_i=1,\ldots,100$) in CR-39 as a function of incident energy E_i, calculating the six polynomial coefficients $c_{\rm in}(Z_i)$ of the expression

$$R_i(Z_i)=\sum_{n=1}^{6} c_{in}(Z_i)[E_i(p_i,A_i)]^n \quad (i=1,2,3). \qquad (1)$$

Since there is no simple relation between track length and fragment charge applicable for the whole range of measured lengths (from 3 μm for the shortest tracks to 400 μm for the longest), we used three different sets of coefficients $c_{\rm in}(Z_i)$ for three different length regions: $R_i<15$ μm, $15\leq R_i\leq50$ μm, and $R_i>50$ μm. Our identification code assigned to each final product the charge Z_i of the ion with deduced momentum p_i and experimental track range R_i compatible with the Eq. (1). The propagation of experimental errors through this procedure implied an estimated mean charge resolution ±1 for those fragments with range longer than 50 μm, ±2 for fragments with tracks $15\leq R_i\leq50$ μm, and ±3 for fragments with track length shorter than 15 μm. Obviously, the main source of systematic uncertainty in the charge determination was the uncertainty of path ranges for the shortest ($R_i<15$ μm) tracks.

The velocity v_i of each fragment was determined from its mass number and momentum with a mean error ±0.2 cm/ns. These velocity values are little affected by light-particle evaporation. Finally, cross sections were calculated with a 10% accuracy by counting the total number of tracks of the incident beam ions directly on the detector surface using a video camera connected to an image analysis computer.

During the course of a heavy-ion collision, the emission of light particles (principally n, p, and α) is a typical process occurring between the initial excitation of the colliding nuclei and the deexcitation of the final products. For the neutron-rich heavy systems and present bombarding energies, reaction products deexcite predominantly by evaporating neutrons or, to a lesser extent, light charged particles ($Z\leq3$) [29]. The measured range R_i for each detected fragment in CR-39 depends on two secondary quantities, its final charge Z_i and its momentum p_i, whilst the momentum values found through the linear momentum conservation equations are primary (or preevaporative) values. The recoil ef-

fects associated with the evaporation (assumed isotropic in the c.m. of the emitting nucleus but not in the lab system) of undetected light particles from the primary fragments, together with the subsequent reduction of the total mass (and charge) available to the final fragments, constitute a source of perturbation in the reconstitution of the kinematics. Thus, due to the effects of limited experimental resolution and light-particle evaporation, momentum conservation is not completely exact for the detected heavy fragments in our reaction. Applying no correction for these effects, in some cases our identification code assigned to the fragments charge values slightly higher than the "real" ones, since for a fixed track length a higher momentum (the preevaporative value) is associated with a higher Z_i (a heavier fragment), leading to a total final Z greater than the sum of the colliding nuclear charges. To overcome this problem, we used an approach similar to the kinematical coincidence method (KCM) [14,30], but instead of requiring the conservation of mass as an additional kinematic constraint on our system, our code assessed iteratively the momentum loss due to the evaporation of undetected light charged particles and neutrons from primary fragments and due to energy loss in the target. This assessment was done by imposing the requirement that the sum of all detected charges in an event not exceed the entrance channel value of 171. This being the case, we subtracted a small contribution from the p_{beam} value of the linear momentum conservation equations (assigning this missing momentum to the emission of undetected light particles and to momentum loss in the target) in an iterative way until satisfying the total charge requirement.

To select events as well characterized as possible, i.e., to reject poorly reconstructed events, we retained only events leading to detection of at least 80% of both the total charge and total parallel momentum in the entrance channel ($Z_{\text{tot}}=171$ and $p_{\text{beam}}=39.95$ GeV/c). Applying this filtering, we rejected about 10% of the initial set, mainly corresponding to incompletely measured events of multiplicity 4 and to events originated from reactions on the CR-39 detector constituents. The mean value of the total detected charge from summing all $Z\geq 8$ fragments for each selected "complete" three-body event was $\langle Z\rangle=168\pm 6$, corresponding to $\approx 98\%$ of the sum of the projectile and target atomic numbers, and the mean total linear momentum along the beam axis in the exit channel was $\langle p_{\parallel}\rangle_{\text{tot}}=36.5$ GeV/c (about 90% of p_{beam}).

III. EXPERIMENTAL RESULTS AND INTERPRETATION

A. Multiplicities and cross sections

Figure 1 shows the multiplicity spectrum of nuclei detected in the CR-39 plates, corrected to take into account the incompletely measured events of higher order. Events of multiplicity 2 have also been normalized to subtract contributions from elastic scattering interactions that could be identified by their typical Coulombian-like kinematics. The first remarkable aspect of this plot is the small number of binary events detected in contrast with the results found in analogous very heavy systems at intermediate bombarding energies (such as $^{208}Pb+^{197}Au$ at 29 MeV/nucleon [31]). Our two-body events, which exhaust only about 5% of the measured reaction cross section, can be ascribed essentially to

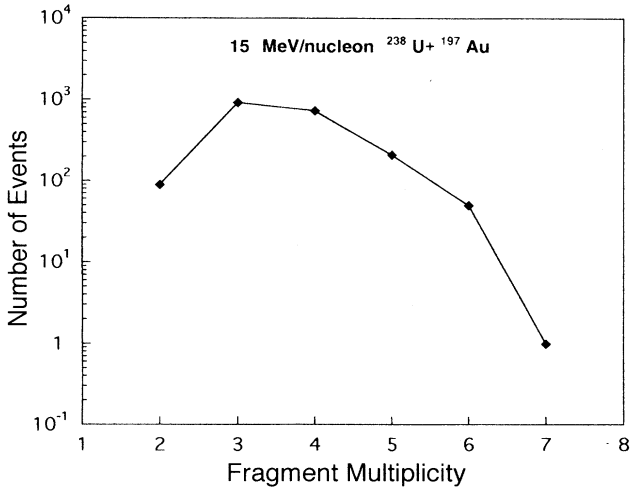

FIG. 1. Experimental fragment multiplicity spectrum of all events in the CR-39 detectors for the reaction studied. This spectrum has been corrected to take into account the incompletely measured events of higher multiplicity.

quasielastic or deep inelastic collisions in which the U-like and Au-like reaction products survive fission after probably evaporating several nucleons.

The three- and four-body events exhaust approximately 83% of the total cross section. In contrast to many other reactions in the Fermi energy domain (see, for example, [16,31,32]), the spectrum does not decrease steeply with increasing multiplicity. Instead, there is a maximum for processes with three heavy final bodies. This effect is due to the fact that we deal with a heavier system in which binary fission of one (or both) reaction partners is an important exit channel as predicted by different statistical models: the Berlin model [33] and the GEMINI code [34]. ^{238}U undergoes fission even at low excitation and thus it is expected that a considerable fraction of the reactions would have at least three heavy nuclei in the exit channel. In the present work we will not study the origin of quaternary events since our kinematic reconstruction method does not provide a unique solution to their kinematics without an extra constraint.

An interesting aspect of our investigated reaction is that, in spite of the moderate excitation energies available in our system ($E^{*}_{\text{max}}\approx 2.2$ MeV/nucleon), events with a multiplicity M_f of up to six and even seven heavy fragments are observed. These multifragment exit channels are presumably due to more central collisions after a series of successive sequential binary decays of the two excited heavy primary nuclei. This mechanism is indicated by kinematic correlations between final fragments in other systems at Fermi energies [35]. The observation of such complex processes at lower Fermi energies, where one would expect a smooth transition from the typical behavior of low-energy binary reactions, confirms first that the multiplicity associated with a heavy-ion reaction rises with increasing masses of projectile and target. However, due to the low statistics for the $M_f=5$, 6, and 7 events (which occur with a combined probability around 13%), the analysis presented below will be centered

TABLE I. Absolute and relative cross sections measured for heavy fragments ($Z \geq 8$) in the reaction 15 MeV/nucleon $^{238}U+^{197}Au$.

Final fragments	σ (mb)	$\sigma_{partial}/\sigma_{total}$ (%)
2	220±80	4.6±2.0
3	2200±200	45.8±4.2
4	1740±300	36.3±6.2
5	520±150	10.8±3.1
≥6	120±50	2.5±1.0
Total	4800±400	100.0±8.4

on three-body events, for which we have better statistics and for which we can make a comparison with other results.

The partial cross sections for the processes with multiplicities 2 to 7 observed in our reaction are listed in Table I. The experimental value of the total cross section obtained summing all partial cross sections amounts to $\sigma_{tot}=4800\pm400$ mb, in good agreement with the geometrical value

$$\sigma_R = \pi R_{int}^2 \left(1 - \frac{V_{Coul}}{E_{c.m.}}\right) \approx 4900 \text{ mb},$$

where $R_{int}=1.16(A_{proj}^{1/3}+A_{targ}^{1/3}+2)$ fm$\approx$16 fm is the interaction radius of the reaction.

B. Charge-velocity correlations in ternary events

The main features of the ternary events can be seen by examining the charge-velocity plot of the reaction. Figure 2 shows the Z versus v/v_{proj} (v being the fragment lab velocity, and the beam velocity $v_{proj}\approx5.3$ cm/ns) two-dimensional contour plot for the heavy fragments detected in the ternary processes. One can distinguish two regions. First, a projectile-like fragment domain with fast ($v/v_{proj}>0.7$) nuclei of intermediate atomic numbers ($30\leq Z\leq70$) with a maximum at about half the projectile charge, and second a region with slow-moving ($v/v_{proj}\approx0.25$) heavier charges ($60\leq Z\leq85$) that is more concentrated at $Z\approx66$ and 77 and easily identified as targetlike evaporation residues. This contour diagram indicates that our reaction, in its first step, proceeds principally via a binary process between the two colliding nuclei.

Hereafter, in order to facilitate the presentation of the data, in each recorded three-body event the fragments will be labeled "fast" (subscript 1), "intermediate velocity" (subscript 2), and "slow" (subscript 3) according to their velocity, assuming that the fastest and slowest nuclei normally

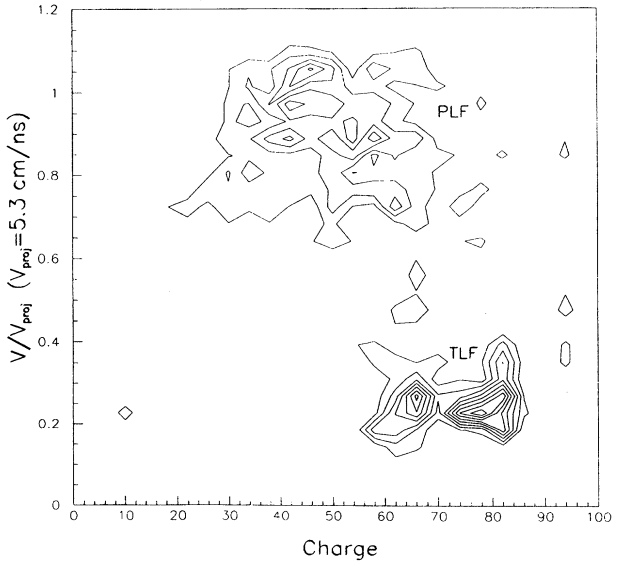

FIG. 2. Two-dimensional contour plot of Z versus v/v_{proj} ($v_{proj}=5.3$ cm/ns is the projectile velocity) spectrum of all heavy fragments ($Z\geq8$) detected in ternary events. PLF stands for projectilelike fragment and TLF for targetlike fragment.

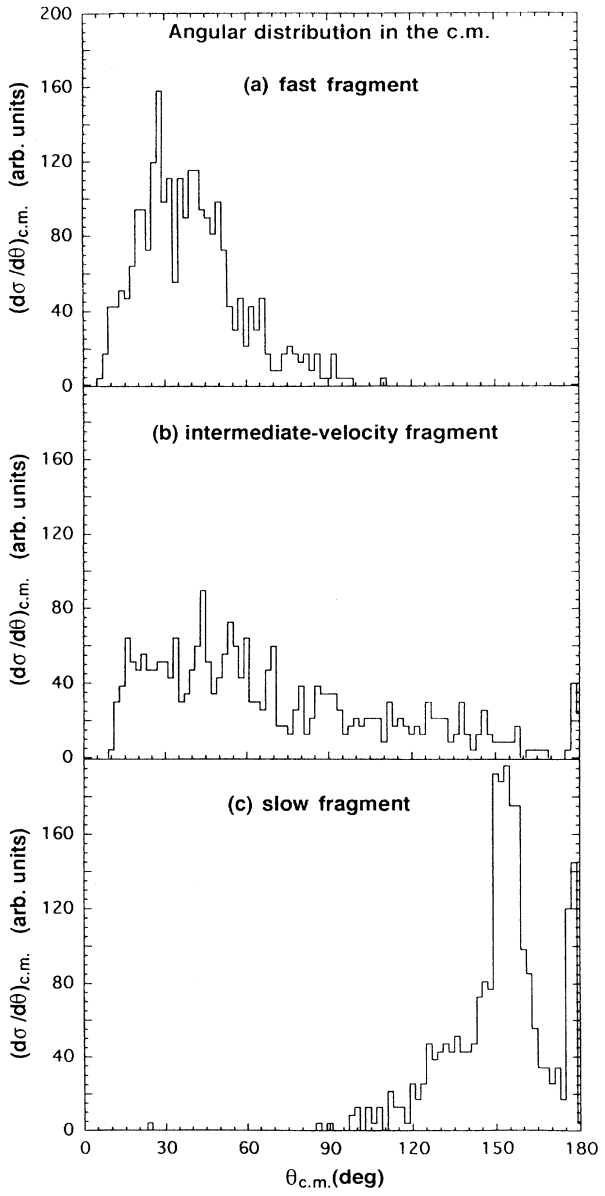

FIG. 3. Angular distributions in the c.m. relative to the beam direction for (a) fast, (b) intermediate-velocity, and (c) slow fragments.

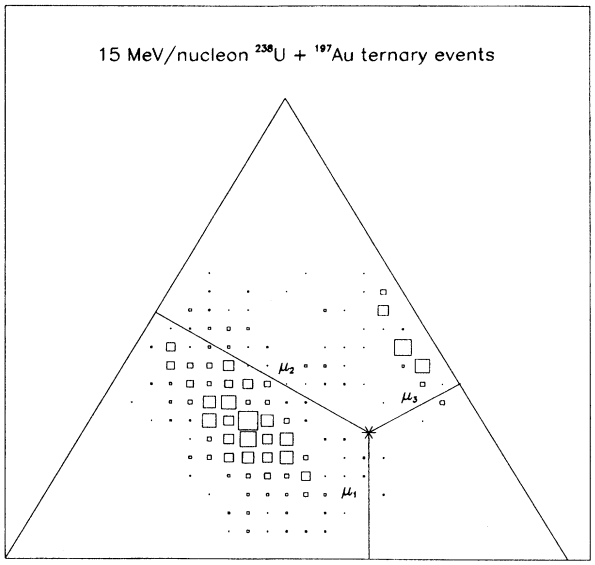

FIG. 4. Dalitz plot for the charge distributions of three-body events issuing from the reaction $^{238}U+^{197}Au$ at 15 MeV/nucleon. The fragment charges Z_i are normalized to the total detected charge in each event. The labels $i=1$, 2, and 3 refer to the fast, intermediate-velocity, and slow final fragments, respectively.

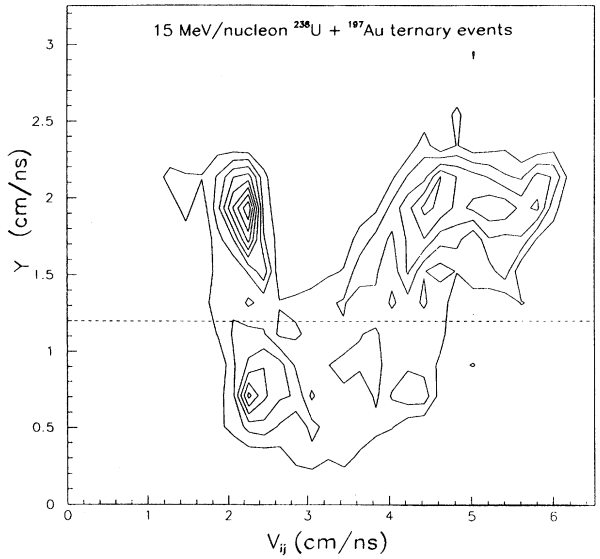

FIG. 5. Two-dimensional contour plot of $Y=\langle v_{rel}\rangle-(v_{rel})_{min}$ versus relative velocities for ternary events in the $^{238}U+^{197}Au$ reaction at 15 MeV/nucleon. For each event, three points are plotted for the same value of Y.

issue from the quasiprojectile and quasitarget, respectively. Quite often, however, the difference in velocity between the fast and intermediate-velocity products is small.

C. Angular distributions in ternary events

The two main reaction products components (fast and slow) found in Fig. 2 differ also in their angular distributions. Figure 3 presents the angular distribution in the c.m. frame for the three detected fragments of different velocities. The angular distributions of the fast [Fig. 2(a)] and intermediate-velocity nuclei [Fig. 2(b)] show forward peaking centered slightly under or on the grazing angle of 29°. That of the slowest fragments [Fig. 2(c)] shows backward peaking. These angular distributions are consistent with peripheral or midperipheral inelastic collisions with projectilelike fragments (the two fastest nuclei) going forward and slow Au-like fragments going backward in the c.m. Nevertheless, the fact that the intermediate-velocity fragment angular spectrum broadens towards more backward angles contrasting with the fast fragment behavior suggests that it probably originates from the part of the projectile most affected by the target interaction.

These figures suggest a typical ternary event in which the two fastest fragments emitted at forward angles seem to be produced by the binary splitting of the quasiprojectile, whereas the slowest fragment is a targetlike nucleus that recoils at lower velocity with a small momentum transferred in its noncentral interaction with the incident uranium.

D. Dalitz plot for charge correlations

For ternary events the initial binary nature of the events is confirmed by the analysis of the charge partition among the three detected fragments. Figure 4 presents the experimental three fragment charge distributions in the form of a Dalitz-type triangular two-dimensional plot based on the conservation of charge $\Sigma_{i=1}^{3}\mu_i=1$ where $\mu_i=Z_i/Z_{tot}$ correspond to the individual fragment charges normalized to the total detected charge of each event. Each fraction μ_i $(i=1,2,3)$ is represented by a point inside the equilateral triangle, with the perpendicular distances to the three sides proportional to the charge fractions μ_i. This plot shows an important clustering of events inside the region determined between the mean charge fraction values: $\langle\mu_1\rangle=0.29\pm0.08$, $\langle\mu_2\rangle=0.26\pm0.08$, and $\langle\mu_3\rangle=0.45\pm0.05$. These fractionations imply an average total charge sharing between the three detected fragments centered at a most probable charge split $\langle Z_1\rangle=49\pm14$, $\langle Z_2\rangle=44\pm14$, and $\langle Z_3\rangle=77\pm9$. This result is clearly compatible with the supposition that the slowest fragment corresponds principally to a recoiling quasi-Au evaporation residue ($\langle Z_3\rangle\approx77$), while the two fastest products would originate in the binary scission of the quasiprojectile ($\langle Z_1\rangle+\langle Z_2\rangle\approx92$) along a quite wide spectrum of charge asymmetries with a maximum centered at half the projectile atomic number (from $Z_1\approx36$ and $Z_2\approx57$ to $Z_1\approx62$ and $Z_2\approx31$ in the most populated region of the Dalitz plot). These correlations between the measured charges of the three fragments show in another way that the primary step of the reaction is predominantly binary.

E. Estimation of impact parameter

At first glance, an event-by-event analysis of Fig. 2 would indicate that about 95% of the ternary processes are peripheral events, i.e., events characterized by the presence of at least one projectile like fragment (defined as any final product with velocity higher than $0.75v_{proj}$). The partition of the ternary events into peripheral and central, however, is not so immediate and must be done using other global variables.

For each event we determine the so-called Y variable [36] which measures the maximum dispersion of the three relative velocities between final fragments with respect to their mean value: $Y=\langle v_{\rm rel}\rangle-(v_{\rm rel})_{\rm min}$. For a given ternary event, a low value of Y indicates a low dispersion of relative velocities which is evidence of a common source for all detected fragments, i.e., of a central collision. On the other hand, a large value of Y, i.e., a large dispersion of final relative velocities, implies the presence of targetlike and projectilelike fragments typical of more peripheral interactions.

Figure 5 shows the two-dimensional spectrum of Y plotted versus the three relative velocities between pairs of detected final fragments in the ternary events. We can separate two regions by the $Y\approx1.2$ cm/ns line. The upper zone ($Y>1.2$ cm/ns), more densely populated, corresponds to the peripheral or semiperipheral collisions while the lower part ($Y<1.2$ cm/ns), less populated, is associated with the central collisions. Approximately 65% of the ternary events fall in the $Y>1.2$ cm/ns zone, where we clearly observe two branches, each one linked with a different emission source for the final fragments. The narrower branch peaks at $v_{ij}=2.3$ cm/ns relative velocity, which is the two-body Coulomb repulsion value expected for fragments following Viola's systematics for the fission of a U-like or Au-like nucleus [37]. The broader branch, centered around $v_{ij}=5$ cm/ns, corresponds to the relative velocity of a fast fragment with respect to another slow one. For $Y<1.2$ cm/ns the three relative velocities also peak at about $v_{ij}=2.3$ cm/ns suggesting that even for more central collisions at least two final fragments arise from a fissionlike process.

The measured threefold events can thus be classified as being produced in reactions where the impact parameters are mainly noncentral and where a fissionlike process of one of the primary fragments appears to be an important decay mechanism at some subsequent stage of the reaction.

F. Energy dissipation

The total kinetic energy (TKE) of the final heavy products in the c.m. system for each ternary event is usually deduced assuming a binary process in the first step of the reaction with the decay of one of the two primary fragments in the second step. After identifying which pair of final fragments originated from the decay of the same primary species (quasiprojectile or quasitarget), we determined the relative velocity $V_{\rm rel}$ between the two heavy partners after separation, knowing that subsequent light-particle evaporation does not affect, on the average, the fragment velocity vectors. The TKE in the c.m. frame was then calculated by $\mathrm{TKE}=0.5\,\mu V_{\rm rel}^2$, where $\mu\approx108$ is approximately the reduced mass of the dinuclear composite system just before separation.

Figure 6 shows the experimental final kinetic energy spectrum for the three-body processes detected in our reaction. This spectrum covers a broad range of exit channel total kinetic energies from the dissipative (400<TKE<900 MeV) into the partially damped (900<TKE<1300 MeV) and then quasielastic regions (1300<TKE<1600 MeV). To explain the observed TKE spectrum one must consider the existence of a dissipative step responsible for a kinetic energy loss in a significant fraction of the ternary processes.

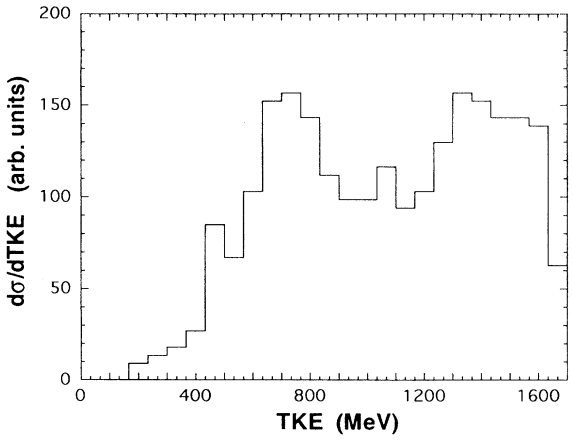

FIG. 6. Reconstructed total kinetic energy (TKE) spectrum of three-fragment events in the exit channel of the reaction.

The difference between the total kinetic energy in the entrance channel ($E_{\rm c.m.}=1.62$ GeV) and that of the final fragments (TKE), i.e., the so-called "total kinetic energy loss" (TKEL) or dissipated kinetic energy, has been shown to be one of the most relevant quantities for determining the production of three-body (and higher-multiplicity) processes in nucleus-nucleus collisions at Fermi energies [14,16,38]. Usually, the TKEL is interpreted as a measure of the excitation energy (thermal and compressional) produced in the reaction. Knowing that the energy loss due to preequilibrium emission in very heavy systems is negligible [31,39], the TKEL can be transformed into excitation energy per nucleon of the system by the following expression: $E^*(\mathrm{MeV/nucleon})=\mathrm{TKEL}/(A_{\rm U}+A_{\rm Au})$. Although we do not observe a complete damping of the entrance channel kinetic energy in our reaction as seen in low-energy very-heavy-ion reactions, according to the former formula, a maximum value $E^*\approx2$ MeV/nucleon corresponding to a temperature $T\approx4$ MeV [according to $E^*=(A/8)T^2$] is reached for some of our threefold events. The energy analysis of the exit channels in ternary processes supports the conclusion that they arise mainly from the binary decay of one of the primary products formed during a first deep inelastic or quasielastic reaction step.

G. Fission properties of ternary events

Up to this point we have considered the correlations between variables that characterize principally the first stages of the reaction. Now we focus on the mechanism that leads to the production of ternary events. As seen in Sec. III E, the relative velocities between the final fragments are some of the most significant observables from which insight into the reaction mechanism can be drawn. A relative velocity analysis (Y variable analysis) of reaction products has already allowed us to distinguish peripheral collisions from central ones and can now help us to identify the existence of any fissioning process. The three relative velocity spectra between each pair of final fragments for ternary processes are presented in Fig. 7. The narrow distribution of v_{12} is clearly peaked at velocities around Viola's value for two fragments produced in the conventional low-energy binary fission of a very heavy nucleus ($A>220$). Considering $v_{\rm Viola}\approx2.3\pm0.3$

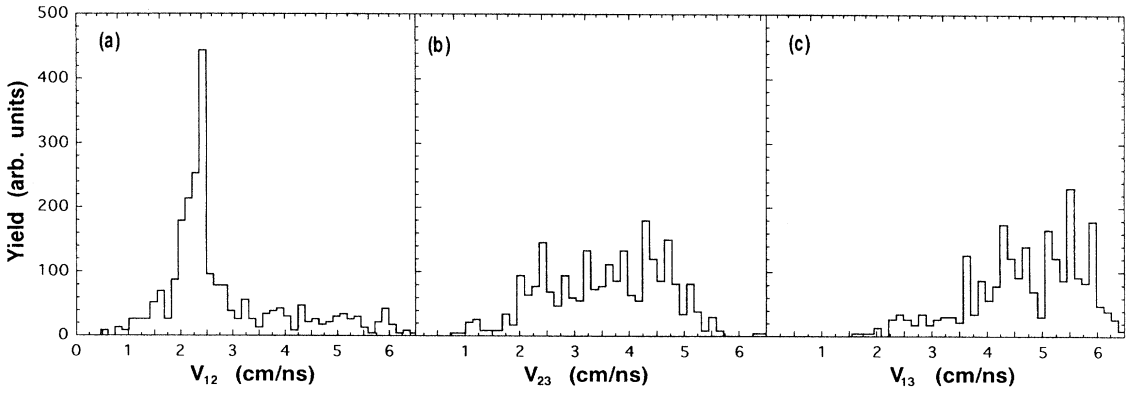

FIG. 7. Relative velocities between (a) the two fastest fragments, (b) the two slowest fragments, and (c) the fastest and slowest fragments.

cm/ns, about 55% of the ternary events have v_{12} compatible with this value. This fact lends support to the idea that the two fastest fragments originate mostly in the sequential fission of the quasiprojectile. The wider distributions of relative velocities v_{23} and v_{13} reflect mainly the initial velocity of separation between quasiprojectile and quasitarget. The v_{23} spectrum between the two slowest nuclei, however, shows a small peak around v_{Viola} for about 15% of three-body processes, indicating that some of them also arise from the fission channel of a quasi-Au in the collisions in which the quasiprojectile survives fission. As expected by fissility arguments, the gold nucleus needs a higher (linear and angular) momentum transfer to fission as compared to the quasi-U nucleus, which fissions with low excitation energy in more peripheral reactions. However, due to the effect of the moderated excitation energy present in the system, the charge distribution of the fissioning fragments is centered around symmetric division in contrast with the asymmetric and double-humped fission charge distribution of "cold" spontaneous or low-energy-induced fission processes.

The total fission cross section represents thus about 70% of the cross section for processes of multiplicity 3 in our reaction and, presumably, also an important part of four-body exit channel processes as observed in [40]. This value is higher than the fission cross section found in other very heavy systems in the intermediate-energy region (such as the 29 MeV/nucleon $^{208}Pb+^{197}Au$ reaction [41]). In this latter work, fission of the quasiprojectile occurred also for rather peripheral collisions but exhausted no more than 20% of the reaction cross section for ternary events. Our data like the data of [41], typical of a sequential emission process, exclude the existence of a prompt multifragmentation process as observed in other reactions in the Fermi energy regime.

In summary, the event-by-event relative velocity analyses for ternary processes (Y-v_{ij} correlations and v_{ij} distributions) suggest a type of event consistent (in about 70% of the original threefold sample) with the emission of a quasitarget in coincidence with two fission projectilelike fragments (about 55% of ternary cases) or of one quasiprojectile and two fission targetlike nuclei (about 15% of the three-body processes) after a first dissipative or a quasielastic binary reaction step.

H. Reconstruction of the first reaction step

For those three-body events where the existence of a fissionlike process was identified unambiguously, we reconstructed the original charges of the primary deep inelastic fragments in order to study the characteristics of the first binary step of our reaction. Since the deexcitation of the excited fission products is dominated by the evaporation of neutrons, the use of $Z_{\text{fiss}}=Z_1+Z_2$ as the charge of the fissioning system is a good approximation [42]. The distribution of the reconstructed charge of the original fissioning composite $Z_{\text{fiss}}=Z_1+Z_2$, where Z_1 and Z_2 are all charges separating with a velocity compatible with Viola's systematics, is shown in Fig. 8. It is found to have a clear maximum centered at the atomic number of the projectile, $Z_{\text{fiss}}\approx 92\pm 3$, with a long tail towards higher Z up to 110 ± 10. More than 60% of the fissioning fragments have a charge higher than that of the projectile ($94<Z_{\text{fiss}}<120$). The reconstructed Z distribution of each coincident primary nonfissioning partner is also shown in Fig. 8. It is concentrated at $Z\approx 80\pm 3$ and 64 ± 3 values. The first peak corresponds to the target atomic number and the second peak to the quasitarget Z value after losing about 16 charge units (by transfer to the projectile

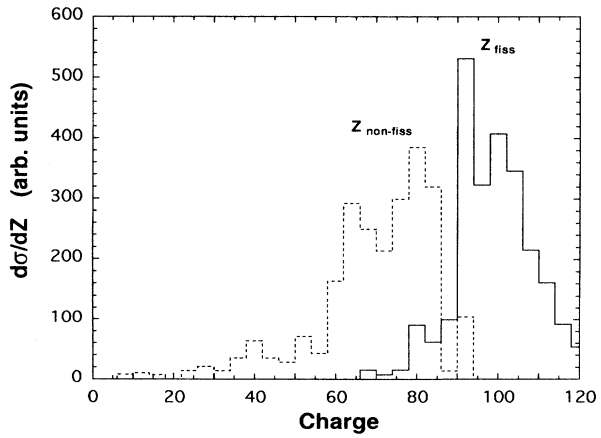

FIG. 8. Reconstructed primary charge of the fissioning composite nucleus Z_{fiss} and detected charge of the nonfissioning fragment Z_{nonfiss}.

and/or subsequent evaporation of undetected light nuclear fragments of $Z<8$ in the deexcitation process). Thus in three-body events, the mean charge of the fissioning composite nucleus ($\langle Z_{\rm fiss}\rangle=97\pm10$) is 5 charge units heavier than the original charge of the projectile (and taking account of undetected light-charged-particle evaporation would increase $Z_{\rm fiss}$). Since the fission probability is larger when the deep inelastic product gains nucleons with respect to the case in which it loses nucleons, both the increased charge (and mass) of the ^{238}U nucleus and its overproportional share of the available excitation energy favor the scission of this primary reaction product in our reaction. The less fissile and excited target remnant, on the other hand, decays by light-particle emission into fragments that are too light to have a significant fission branch.

One interesting aspect of our analysis is that the exit channel of the first binary step in our ternary events shows a higher charge asymmetry than the initial entrance channel configuration. Figure 8 demonstrates that the net transfer of protons from the targetlike to the projectilelike fragment is favored, leading to a small drift towards mass asymmetry. This is evidence of the absence of a true formation of a totally equilibrated dinuclear composite system during the prefission stage and, indirectly, a qualitative indication that the interaction time between the colliding nuclei is not sufficiently long to attain thermal equilibrium and to completely damp the incident kinetic energy of the system. This behavior is in disagreement with the trends observed in several other very-heavy-ion reactions at low energies interpreted in terms of a "quasifission" reaction mechanism such as those observed in ^{238}U-induced reactions on lighter targets ($16\leqslant Z\leqslant 48$) [43]. In those experiments one finds that mass drift towards symmetry takes place in reactions where the relative motion of the interacting nuclei has been completely damped. Both effects, typical signatures of a "quasifission" process, are not present in our reaction which reveals characteristics more related with partially damped deep inelastic scattering processes.

Mass distributions of fragments produced in dissipative heavy-ion reactions can be described classically by a transport equation of the Fokker-Planck type [44]. We can consider the mass transfer process between projectile and target by comparing our experimental data with the quantitative predictions of the Fokker-Planck equation applied to the colliding 15 MeV/nucleon ^{238}U+^{197}Au system. Indeed, the observed net mass drift of some nucleons from target to projectile is confirmed by using a one-dimensional Fokker-Planck equation of the form

$$\frac{\partial}{\partial t}P(A_{\rm proj},t)=\frac{\partial}{\partial A_{\rm proj}}[\nu(A_{\rm proj},t)P(A_{\rm proj},t)]+\frac{\partial^2}{\partial A_{\rm proj}^2}[D(A_{\rm proj},t)P(A_{\rm proj},t)],$$

which describes the distribution of the probability function $P(A_{\rm proj},t)$ for the mass ($A_{\rm proj}$) of the quasiprojectile after the first reaction step. For very short interaction times ($t\approx6\times10^{-21}$ s) the solution has a Gaussian form:

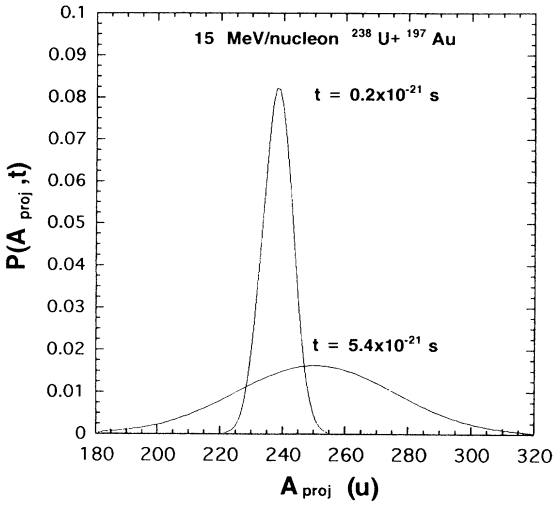

FIG. 9. Solution of the Fokker-Planck equation for three-fragment exit channels.

$$P(A_{\rm proj},t)=\frac{1}{\sqrt{4\pi Dt}}\exp\left[\frac{-(A_{\rm proj}-(A_{\rm proj})_0-\nu t)^2}{4Dt}\right],$$

where the calculated drift ($\nu_A=2.33\times10^{21}$ u/s) and diffusion ($D_A=5.75\times10^{22}$ u^2/s) coefficients are assumed to be constant during the estimated interval of time $t=5.4\times10^{-21}$ s of the first reaction step. Figure 9 shows the solution of the Fokker-Planck equation for our reaction. The maximum of the $P(A_{\rm proj},t)$ distribution peaks at $A_{\rm proj}\approx238$ just at the beginning of the process and at $A_{\rm proj}\approx251$ for $t=5.4\times10^{-21}$ s, i.e., there is a net mass drift from target to projectile of about 13 nucleons. This simple transport model calculation confirms semiquantitatively the experimentally observed 5-charge-units mean increase of the projectile charge after the dissipative interaction with the target.

IV. SUMMARY AND CONCLUSIONS

Events with fragment multiplicities ($Z\geqslant8$) up to 7 have been detected using CR-39 solid state nuclear track detectors in the reaction ^{238}U+^{197}Au at 15 MeV/nucleon. The present study has focused on the identification of events leading to the production of three heavy fragments in the exit channel in which more than 80% of both total charge and parallel linear momentum were detected. For each ternary process, an analysis of the measured geometrical parameters (ranges and angles) of all detected fragments allows the determination of other reaction parameters (charges, velocities) assuming linear momentum conservation after estimating the minimal linear momentum loss due to light-particle evaporation and energy loss in the target.

The measured total cross section for the reaction amounts to $\sigma_{\rm tot}=4800\pm400$ mb, in good agreement with the geometrical cross section $\sigma_R\approx4900$ mb. The fragment multiplicity (M_f) distribution reveals the existence of several decay modes for the system. It first supports the conclusion that for a system as heavy as ^{238}U+^{197}Au, the binary collisions ($M_f=2$) with eventual light-particle evaporation represent a

possible decay mode only for the gentlest collisions in contrast to what happens with similar systems at lower or similar energies. Binary fission of one (U-like) or both (U-like and Au-like) damped primary products clearly dominates for peripheral and intermediate impact parameters (M_f=3 and 4, which exhaust more than 80% of the total cross section). Multifragment emission sets in for the most central collisions with an important emission of complex fragments (up to M_f=7 where $Z \geq 8$ have been detected) even if the maximum excitation energy produced in our system does not exceed 2 MeV/nucleon.

A detailed analysis of three-body events confirms, as reported in similar experiments [16], that the reaction $^{238}U+^{197}Au$ at 15 MeV/nucleon proceeds mostly via a sequential two-step mechanism: an initial peripheral or midperipheral projectile-target interaction (in about 65% of the threefold sample) plus a deep-inelastic-like binary process followed by the subsequent symmetric fissionlike decay of the quasiprojectile and light charged particle and neutron evaporation of the quasitarget. The relative velocity between the two fastest fragments is strongly peaked at values close to the predictions of the Viola systematics for the conventional sequential fission of a very heavy nucleus ($A>220$) in about 55% of the ternary events. These results rule out the possibility of a prompt multifragmentation process as observed at higher energies. The total fission cross section, summing quasiprojectile and quasitarget fissions, represents about 70% of the total three-body exit channel cross section.

The reconstructed charges of the primary deep inelastic fragments indicate that there exists a net transfer of nucleons from target to projectile. This is evidence of the formation of a nonequilibrated dinuclear system during the first stage of the reaction, in disagreement with the results found in low energy "quasifission" reactions with very heavy ions.

In conclusion, our very heavy system reveals typical features expected in both the low- and high-bombarding-energy regimes. While the reaction mechanism of the most important exit channel (three-body processes) is entirely consistent with a low-energy point of view (deep inelastic dynamics plus sequential fission and light-particle evaporation) in agreement with similar investigations at Fermi energies, the observation of a mass drift that increases the initial entrance channel charge asymmetry configuration implies that there is no true formation of a completely equilibrated dinuclear composite system during the first binary reaction step. This observation is at odds with the typical "quasifission" results observed in lower-energy very-heavy-ion reactions [43]. Finally, the fragment multiplicity M_f distribution shows the presence of a multifragment component (M_f=5, 6, and 7) characteristic of higher-bombarding-energy behavior.

ACKNOWLEDGMENTS

The authors wish to express their appreciation to the staff of the GSI UNILAC and especially to J. Vetter for performing the irradiations. We also thank L. Oberlé for careful measuring and A. Pape for very useful discussions.

[1] D. Hilscher and H. Rossner, Ann. Phys. (Paris) **17**, 471 (1992).

[2] J. Töke, R. Bock, G. X. Dai, A. Gobbi, S. Gralla, K. D. Hildenbrand, J. Kuzminski, W. F. J. Müller, A. Olmi, H. Stelzer, B. B. Back, and S. Bjørnholm, Nucl. Phys. **A440**, 327 (1985).

[3] H. Freiesleben, K. D. Hildenbrand, F. Pühlhoffer, W. F. W. Schneider, and R. Bock, Z. Phys. A **292**, 171 (1979).

[4] M. Schädel, W. Brüchle, H. Gäggeler, J. V. Kratz, K. Sümmerer, G. Wirth, G. Herrmann, R. Stakemann, G. Tittel, N. Trautmann, J. M. Nitschke, E. K. Hulet, R. W. Lougheed, R. L. Hahn, and R. L. Ferguson, Phys. Rev. Lett. **48**, 852 (1982).

[5] H. Backe, P. Senger, W. Bonin, E. Kankeleit, M. Krämer, R. Krieg, V. Metag, N. Trautmann, and J. B. Wilhelmy, Phys. Rev. Lett. **50**, 1838 (1983).

[6] G. Wirth, W. Brüchle, Fan Wo, K. Sümmerer, F. Funke, J. V. Kratz, N. Trautmann, and V. E. Oberacker, Z. Phys. A **330**, 87 (1988).

[7] P. Fröbrich and J. Stroth, Phys. Rev. Lett. **64**, 629 (1990).

[8] G. Beier, J. Friese, W. Henning, P. Kienle, H. J. Körner, W. Wagner, W. A. Mayer, and W. Mayer, Z. Phys. A **336**, 217 (1990).

[9] F. Funke, J. V. Kratz, N. Trautmann, N. Wiehl, G. Wirth, W. Brüchle, F. Wo, and K. Sümmerer, Z. Phys. A **340**, 303 (1991).

[10] G. Wirth, F. Funke, W. Brüchle, Wo Fan, J. V. Kratz, K. Sümmerer, and N. Trautmann, Phys. Lett. B **253**, 28 (1991).

[11] S. S. Sharma and D. Galetti, Phys. Rev. C **45**, 1347 (1992).

[12] J. D. Molitoris, W. E. Meyerhof, C. Stoller, R. Anholt, D. W. Spooner, L. G. Moretto, L. G. Sobotka, R. J. McDonald, G. J. Wozniak, M. A. McMahan, L. Blumenfeld, N. Colonna, M. Nessi, and E. Morenzoni, Phys. Rev. Lett. **70**, 537 (1993).

[13] D. Dalili, R. Lucas, C. Ngô, C. Cerruti, S. Leray, C. Mazur, M. Ribrag, T. Suomijärvi, M. Berlanger, S. Chiodelli, A. Demeyer, and D. Guinet, Nucl. Phys. **A454**, 163 (1986).

[14] A. Olmi, P. R. Maurenzig, A. A. Stefanini, J. Albinski, A. Gobbi, S. Gralla, N. Hermann, K. D. Hildenbrand, J. Kuzminski, W. F. J. Müller, M. Petrovici, H. Stelzer, and J. Toke, Europhys. Lett. **4**, 1121 (1987).

[15] M. Gui, K. Hagel, R. Wada, Y. Lou, D. Utley, B. Xiao, J. Li, J. B. Natowitz, G. Enders, W. Kühn, V. Metag, R. Novotny, O. Schwalb, R. J. Charity, R. Freifelder, A. Gobbi, W. Henning, K. D. Hildenbrand, R. Mayer, R. S. Simon, J. P. Wessels, G. Casini, A. Olmi, and A. A. Stefanini, Phys. Rev. C **48**, 1791 (1993).

[16] R. J. Charity, R. Freifelder, A. Gobbi, N. Herrmann, K. D. Hildenbrand, F. Rami, H. Stelzer, J. P. Wessels, G. Casini, P. R. Maurenzig, A. Olmi, A. A. Stefanini, J. Galin, D. Guerreau, U. Jahnke, A. Péghaire, J. C. Adloff, B. Bilwes, R. Bilwes, G. Rudolf, M. Petrovici, M. Gnirs, and D. Pelte, Z. Phys. A **341**, 53 (1991), and references therein.

[17] G. Casini, A. A. Stefanini, M. Bini, P. R. Maurenzig, A. Olmi, G. Poggi, R. J. Charity, R. Freifelder, A. Gobbi, K. D. Hildenbrand, M. H. Tanaka, and J. P. Wessels, Phys. Rev. Lett. **67**, 3364 (1991).

[18] G. Casini, P. G. Bizzeti, P. R. Maurenzig, A. Olmi, A. A. Stefanini, J. P. Wessels, R. J. Charity, R. Freifelder, A. Gobbi, N.

Herrmann, K. D. Hildenbrand, and H. Stelzer, Phys. Rev. Lett. **71**, 2567 (1993).
[19] O. Granier, C. Cerruti, S. Leray, P. L'Hénoret, R. Lucas, C. Mazur, J. Natowitz, C. Ngô, M. Ribrag, E. Tomasi, G. Imme, G. Racik, G. Spinolla, L. Albinski, A. Gobbi, N. Hermann, K. D. Hildenbrand, and A. Olmi, Nucl. Phys. **A481**, 109 (1988).
[20] P. A. Gottschalk, P. Vater, H. J. Becker, R. Brandt, F. Grawert, G. Fiedler, R. Haag, and T. Rautenberg, Phys. Rev. Lett. **42**, 359 (1979).
[21] C. Bretchmann and W. Heinrich, Z. Phys. A **330**, 407 (1988).
[22] B. Jakobsson, G. Jönsson, L. Karlsson, B. Norén, K. Söderström, F. Schussler, and E. Monnand, Nucl. Phys. **A488**, 251c (1988).
[23] A. Hoffman, C.Bretchmann, and W. Heinrich, Phys. Lett. B **200**, 583 (1988).
[24] C. Bretchmann, W. Heinrich, and E. V. Benton, Phys. Rev. C **39**, 2222 (1989).
[25] M. Zamani, M. Debeauvais, J. Ralarosy, J. C. Adloff, F. Fernández, S. Jokic, and D. Sampsonidis, Phys. Rev. C **42**, 331 (1990).
[26] C. Lewenkopf, J. Dreute, A. Abul-Magd, J. Aichelin, W. Heinrich, J. Hüfner, G. Rusch, and B. Wiegel, Phys. Rev. C **44**, 1065 (1991).
[27] J. Dreute, W. Heinrich, G. Rusch, and B. Wiegel, Phys. Rev. C **44**, 1065 (1991).
[28] J. F. Ziegler and J. M. Manoyan, Nucl. Instrum. Methods Phys. Res. Sect. B **35**, 215 (1989).
[29] E. Piasecki, S. Bresson, B. Lott, R. Bougault, J. Colin, E. Crema, J. Galin, B. Gatty, A. Genoux-Lubain, D. Guerreau, D. Horn, D. Jacquet, U. Jahnke, J. Jastrzebski, A. Kordyasz, C. Le Brun, J. F. Lecolley, M. Louvel, M. Morjean, C. Paulot, L. Pienkowski, J. Pouthas, B. Quednau, W. U. Schröder, E. Schwinn, W. Skulski, and J. Töke, Phys. Rev. Lett. **66**, 10 (1991).
[30] G. Casini, P. R. Maurenzig, A. Olmi, and A. A. Stefanini, Nucl. Instrum. Methods Phys. Res. Sect. A **277**, 445 (1989).
[31] M. Aboufirassi, A. Badala, R. Bougault, R. Brou, J. Colin, D. Durand, A. Genoux-Lubain, D. Horn, J. L. Laville, C. Le Brun, J. F. Lecolley, F. Lefevres, O. Lopez, M. Louvel, M. Mahi, J. C. Steckmeyer, B. Tamain, B. Bilwes, F. Cosmo, G. Rudolf, F. Scheibling, L. Stutgé, S. Tomasevic, J. Galin, D. Gerreau, M. Morjean, A. Péghaire, and D. Jaquet, LPC-Caen Report No. LPCC **93-14**, 1993.
[32] M. Bruno, M. D' Agostino, M. L. Fiandri, E. Fuschini, P. M. Milazzo, A. Cunsolo, A. Foti, F. Gramegna, F. Gulminelli, I. Iori, L. Manduci, A. Moroni, R. Scardaoni, P. Buttazzo, G. V. Margagliotti, G. Vannini, G. Auger, and E. Plagnol, Phys. Lett. B **292**, 251 (1992).
[33] D. H. E. Gross, Nucl. Phys. **A553**, 175c (1993).
[34] R. J. Charity, M. A. McMahan, G. J. Wozniak, R. J. McDonald, L. G. Moretto, D. G. Sarantites, L. G. Sobotka, G. Guarino, A. Pantaleo, L. Fiore, A. Gobbi, and K. D. Hildenbrand, Nucl. Phys. **A483**, 371 (1988).
[35] G. Bizard, D. Durand, A. Genoux-Lubain, M. Louvel, R. Bougault, R. Brou, H. Doubre, Y. El-Masri, H. Fugiwara, K. Hagel, A. Hajfani, F. Hanappe, S. Jeong, G. M. Jin, S. Kato, J. L. Laville, C. Le Brun, J. F. Lecolley, S. Lee, T. Matsuse, T. Motobayashi, J. P. Patry, A. Péghaire, J. Péter, N. Prot, R. Regimbart, F. Saint-Laurent, J. C. Steckmeyer, and B. Tamain, Phys. Lett. B **276**, 413 (1992).
[36] R. Bougault, F. Delaunay, A. Genoux-Lubain, C. Le Brun, J. F. Lecolley, F. Lefebvres, M. Louvel, J. C. Steckmeyer, J. C. Adloff, B. Bilwes, R. Bilwes, M. Glaser, G. Rudolf, F. Scheibling, L. Stuttgé and J. L. Ferrero, Nucl. Phys. **A488**, 255c (1988).
[37] V. E. Viola, K. Kwiatkowski, and M. Walker, Phys. Rev. C **31**, 1550 (1985).
[38] B. M. Quednau, S. P. Baldwin, B. Lott, W. U. Schröder, B. M. Szabo, J. Töke, S. Bresson, J. Galin, D. Guerreau, and M. Morjean, GANIL Compilation 111, 1992–1993.
[39] B. M. Quednau, S. P. Baldwin, B. Lott, W. U. Schröder, B. M. Szabo, J. Töke, D. Hilscher, U. Jahnke, H. Rossner, S. Bresson, J. Galin, D. Guerreau, M. Morjean, and D. Jacquet, Phys. Lett. B **309**, 10 (1993).
[40] J. Ralarosy, M. Debeauvais, J. C. ADloff, M. Zamani, F. Fernandez, S. Jokic, and Z. Todorovic, Nucl. Tracks Radiat. Meas. **19**, 651 (1991).
[41] S. Bresson, M. Morjean, L. Pienkowski, R. Bougault, J. Colin, E. Crema, J. Galin, B. Gatty, A. Genoux-Lubain, D. Guerreau, D. Horn, D. Jacquet, U. Jahnke, J. Jastrzebski, A. Kordyasz, C. Le Brun, J. F. Lecolley, B. Lott, M. Louvel, C. Paulot, E. Piasecki, J. Pouthas, B. Quednau, W. U. Schröder, W. Skulski, and J. Töke, Phys. Lett. B **294**, 33 (1992).
[42] M. Begemann-Blaich, Th. Blaich, M. M. Fowler, J. B. Wilhemy, H. C. Britt, D. J. Fields, L. F. Hansen, R. G. Lanier, D. J. Massoletti, M. N. Namboodiri, B. A. Remington, T. C. Sangster, G. L. Struble, M. L. Webb, Y. D. Chan, A. Dacal, A. Harmon, J. Pouliot, R. G. Stokstad, S. Kaufman, F. Videbaek, and Z. Fraenkel, Phys. Rev. C **45**, 677 (1992).
[43] W. Q. Shen, J. Albinski, A. Gobbi, S. Gralla, K. D. Hildenbrand, N. Herrmann, J. Kuzminski, W. F. J. Müller, H. Stelzer, J. Töke, B. B. Back, S. Bjørnholm, and S. P. Sørensen, Phys. Rev. C **36**, 115 (1987).
[44] H. Freiesleben and J. V. Kratz, Phys. Rep. 106 (1984).